

# BEAM-BASED ALIGNMENT, TUNING AND BEAM DYNAMICS STUDIES FOR THE ATF2 EXTRACTION LINE AND FINAL FOCUS SYSTEM\*

G.R.White, LAL, Univ Paris-Sud, CNRS/IN2P3, Orsay, France & SLAC, CA, USA. S.Molloy,  
M.Woodley, SLAC, CA, USA

## Abstract

Using a new extraction line currently under construction, the ATF2 experiment plans to test the novel compact final focus optics design with local chromaticity correction intended for use in future linear colliders. With a 1.3 GeV design beam of 30nm normalised vertical emittance extracted from the ATF damping ring, the primary goal is to achieve a vertical spot-size at the IP waist of 37nm.

We discuss our planned strategy for tuning the ATF2 beam to meet the primary goal. Simulation studies have been performed to asses the effectiveness of the strategy, including “static” (installation) errors and dynamical effects (ground-motion, mechanical vibration, ring extraction jitter etc.). We have simulated all steps in the tuning procedure, from initial orbit establishment to final IP spot-size tuning. Through a Monte Carlo study of 100's of simulation seeds we find we can achieve a spot-size within ~10% of the design optics value in at least 75% of cases. We also ran a simulation to study the long-term performance with the use of beam-based feedbacks.

## INTRODUCTION

A detailed description of the ATF2 project at KEK can be found elsewhere [1]. The simulation studies presented here were performed in order to estimate the effectiveness of the planned procedures to tune the ATF2 extraction line (EXT) and final focus system (FFS). The ATF2 FFS has been designed as a scaled version of the ILC BDS FFS optics, and the tuning procedures outlined here are applicable to both.

## SUMMARY OF TUNING PROCEDURES

### *Initial Conditions*

As a starting point for the tuning procedures considered in these simulations it is assumed some initial commissioning has already occurred. Namely, that the beam is able to be passed to through to the dump, a survey of magnet locations has been performed, and calibration procedures for the BPMs have been carried out and they are operating with their planned resolution performance expectations.

### *EXT Tuning*

Using the 16 horizontal and 11 vertical corrector magnets and the 23 magnet BPMs in the EXT, a 1-1 steering algorithm is used to steer the beam to an initial orbit. The steering solution is over-constrained and tuned such that the BPM measured orbit is minimised and the integrated correction magnet strength also minimised in a least-squared sense. A weighting technique is used to

ensure an adequate launch into the FFS by biasing the orbit correction in the final few BPMs. This steering system also serves as the pulse-pulse feedback system for the EXT (a gain is applied to the correction vector in feedback mode).

Dispersion correction is performed in the diagnostic section (where the dispersion is arranged to be nominally zero). By scanning the frequency of the main damping ring RF, and hence the beam energy in the EXT, the dispersion at the BPM locations is calculated and back-propagated to the start of the diagnostic section.  $\eta_x$  and  $\eta'_x$  are corrected using QF1X + QF6X quadrupole multi-knobs. Vertical dispersion is corrected using a “sum multiknob” with QS1X and QS2X skew-quadrupoles. Special care was taken to arrange the optics between the skew quads such that no coupling or horizontal dispersion is generated whilst applying this knob.

Coupling correction is performed in the diagnostics section by sequentially scanning the 4 skew quadrupoles and minimising the vertical projected emittances at the associated wirescanner locations (iteratively).

### *FFS Tuning*

The initial orbit is obtained with a combination of the launch system (part of the EXT steering and feedback referred to above) and the FFS feedback which consists of 2 orthogonal pairs of correctors and BPMs in the non-dispersive region for horizontal and vertical corrections.

Next, the quadrupoles are aligned to their BPMs using a quadrupole shunting technique. The quadrupole strengths are changed to 80% of their operating value and returned to normal, taking downstream BPM readings at both settings. The offset between the incoming beam and the magnetic field centre is inferred by the change in the downstream BPM readings. The magnet is then moved to the expected zero field-offset position and the routine is repeated. This is iterated until a zero-crossing is confirmed within the resolution limits of the BPMs and magnet mover system. The magnet mover system is finally returned to its zero-offset position.

Beam-based alignment of the quadrupole magnets is performed using a 1-1 steering algorithm together with the mover system. The algorithm attempts to move all the quadrupole magnets such that the beam passes through the centre of each magnet's BPM. To prevent a solution presenting itself where large magnet moves in the centre of the correction area are present, the moves of the magnets are constrained using a weighting procedure in the matrix inversion process.

The sextupole magnets are to be deactivated during the above procedures. After quadrupole alignment is complete, they are re-activated and moved onto the beam

\*work supported in part by Department of Energy Contract DE-AC02-76SF00515

axis using their attached BPMs. The BPMs are aligned to the magnetic field centre by moving the sextupoles through the beam. This results in a parabolic response in downstream BPMs. The alignment is read-off at the position of zero-gradient from the fitted BPM responses.

A combination of multi-knobs are now iteratively applied to try and tune-out remaining linear and higher-order aberrations at the IP. If the size of the beam is larger than the capture range of the Shintake-monitor ( $<1\text{um}$ ), then initial tuning will have to be performed using one of the other 2 secondary IP-points with different scanners (carbon wirescanner and “nano-pattern” monitor). The main tuning knobs use co-ordinated horizontal moves of the sextupole magnets to tune-out IP waist offset and vertical moves to tune-out dispersion and  $\langle x'y' \rangle$  coupling. The knobs are computed to be orthogonal, but under realistic error conditions they are not completely so and the knobs only converge when applied iteratively. In addition to these knobs which couple to the linear IP aberrations, the roll-axis of the sextupole movers is used to couple to higher-order terms. The most effective use of this was found to be to scan each sextupole in turn, minimising the calculated IP vertical spot size each time. The 4 skew-quadrupoles in the EXT diagnostic section were also used to tune-out the other cross-plane coupling terms at the IP. These provided only a marginal improvement as the majority of the coupling is introduced via the  $\langle x'y' \rangle$  term dealt with using the sextupole multi-knobs.

## SIMULATION OF TUNING PROCEDURE

A simulation encompassing all of the above procedures including realistic error conditions was written to test the ability to tune to close to the desired vertical beam size at the nominal IP position. The simulation was written in Matlab using the Lucretia accelerator modelling toolbox. V.3.7 of the ATF2 optics was used, and read-in from the standard XSIF deck. Results were obtained by tracking a 10K macro-particle representation of the beam. Because of the non-linear nature of the final focus optics, the vertical beam profile at the IP deviates from a perfect gaussian shape. The spot size is calculated by fitting a gaussian profile to the core of the beam. A simple RMS estimate of the beam size has a considerable contribution from the non-gaussian tails in the vertical distribution making it an inappropriate metric. In a colliding accelerator, it is this gaussian fit that most represents the operating luminosity so this is a valid performance metric for the case of ATF2.

For the results of the simulation shown below, 100 random seeds were used, where the different seeds mean different patterns of applied static and dynamic errors and starting conditions for the ground motion simulation.

### Static Errors

These are the error sources used in the model to account for differences in the initial condition of the accelerator to that expected in the model (survey resolution limits, magnetic strength errors etc). All errors are applied with a gaussian distribution with shown RMS values.

- x/y/z Magnetic alignment errors: 200um
- Roll tolerances: 300urad
- Initial BPM-magnet alignment: 30um
- Magnetic field tolerances: dB/B 1e-4 systematic + 1e-4 random
- Power supply resolution: 16-bit controllers

The magnetic field tolerances are quoted in 2 parts- the first part deals with a systematic measurement/installation error on all magnets, the second is a random fluctuation on a per-magnet basis.

Computed higher-order field components for the 3 FFS bend magnets and measured ones for the final quadrupole doublet are used.

### Dynamic Errors

The ATF2 error sources that have a dynamical component are listed here. Although these ‘jitter sources’ have an insignificant direct effect on beam size at the IP when counteracted with beam-based feedbacks, the residual position jitter at the IP affects the accuracy of the beam size measurement by the Shintake monitor. It is not feasible to simulate the ATF2 operation on a pulse-by-pulse basis over the whole tuning convergence time. Instead, the effect of the dynamic errors on the beam size measurement are added in quadrature to the expected measurement resolution of the Shintake monitor. For the values quoted here, the calculated effect is to add 1.3nm of jitter to the 2nm measurement resolution expected, giving a 2.4nm RMS resolution for this device in simulation. Errors are applied with a normal distribution weighting with the shown RMS values:

- $0.1\sigma_{x,x',y,y'}$  ring extraction jitter
- 10 nm magnet vibration
- 1e-4 strength errors pulse-pulse on corrector magnets
- 100 nm BPM resolution

Additionally, a ground motion model is applied. The ground motion model is based on a fit to data taken at KEK on the ATF floor.

The most sensitive error parameter is that for magnet vibration- especially for the final doublet which strongly correlates to motion of the beam at the IP. The next most sensitive parameter is that for corrector strength fluctuation, which starts to dominate the dynamic cause of IP beam size growth if the error parameter is more than doubled from that shown here.

### IP Beam Size Measurement and Feedbacks

The primary method of measuring the beam size at the IP is with the Shintake monitor (interference fringe laser system) [2]. The specifications for this system state that a measurement of the beam size with an accuracy of 2nm is possible by sweeping the laser waist past the beam over 90 consecutive pulses. In the simulation, each beam size measurement is taken with a random error of 2.4nm to allow for the additional error from dynamical sources. After each measurement, 90 pulses at 1.56 Hz (about 1min) of ground motion is applied to the beamline. The beam trajectory is maintained using the EXT and FFS steering systems described above. To operate both simultaneously without too much interference, the EXT

system is operated with 1/10 the gain of the FFS system. This gives a correction to a step disturbance in about 20 pulses, which is enough to maintain an orbit correction that doesn't degrade the beamsize on a short timescale. The FFS feedback is operated with higher gain as the tolerances are much tighter in this region. Figure 4a shows that with the feedbacks operating there is a steady beam size growth of about 0.5nm an hour on average.

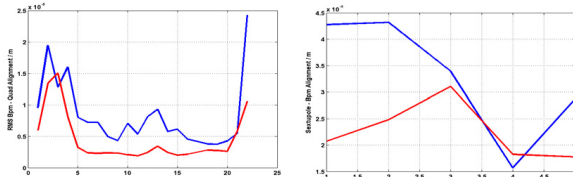


Figure 1: Alignment of Quadrupole and Sextupole Magnets to their BPMs (red= vertical blue=horizontal)

Figure 4b shows that with periodic retuning (application of linear and higher-order sextupole multi-knobs), this is mitigated. The growth is mainly due to orbit drift in the FFS sextupoles as there is not the possibility of maintaining the orbit fixed in each one using correctors. Depending on the stability/accuracy of the mover system and relative alignment stability of the sextupole BPMs, it may be possible to also partially mitigate this effect by tracking the orbit drifts with the magnet movers.

#### Dynamic Range of Magnet Mover System

Details of the mover system can be found elsewhere [3]. The movers have a given phase-space of allowable motion in x/y/roll – the more motion in one axis, the less is available in the other two. A calculation was made at each step of the simulation to see if we move outside of the allowed range. Of the 100 seeds simulated; 14 limit checks failed during the initial steering; 10 during the quadrupole alignment process; and 4 during the sextupole

multi-knob tuning. The 24 failures during initial steering and alignment need to be fixed through the use of tighter restrictions on allowed magnet moves. For the failures in the final tuning stage, the system would need to be re-aligned, fortunately this has only happened in 4% of the seeds.

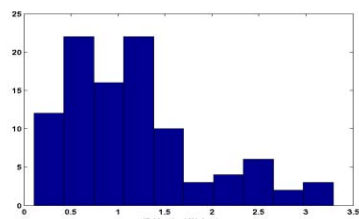


Figure 2: IP Vertical beam size after alignment and steering (100 seeds)

## SIMULATION RESULTS

The results shown here should be compared to the calculated IP vertical beam size of 37.4nm when tracked with an error-free model. Figure 1 shows the results of the simulated quad shunting and sextupole BPM alignment simulations. The alignment is better than 10um for the quads and 4um for the sextupoles. The variance between the magnets arises from the differing numbers of

downstream BPMs to use and the differing phase advances available.

The tuning simulation corresponds to a real-time period of about 8 days. The sextupole multi-knobs were applied

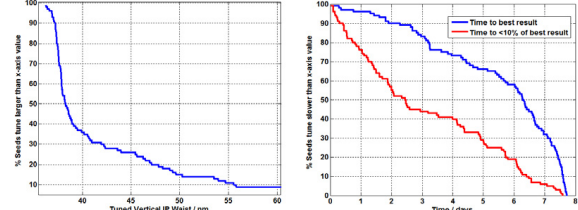


Figure 3: Percentage of seeds that tune to better than the size given on the y-axis and the convergence time.

iteratively using a 1-d parabolic optimiser to find the smallest spot size for each knob being scanned. The initial beam sizes for the 100 seeds before sextupole tuning (post alignment and orbit steering) are shown in figure 2.

The vertical IP beam size quickly tunes to below ~100nm, but very slowly converges after that in many cases due to the random fluctuation of the IP measurement and loss of orthogonality of the knobs. Figure 3 summarises the final spot size found and the time taken for convergence.

For the results shown in figures 4a and 4b, one seed was evolved in time with dynamic error sources and feedback applied (repeated with 100 different random seeds for the time-based evolution).

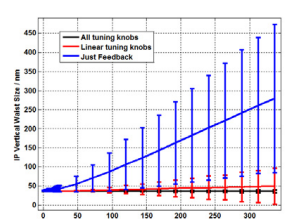
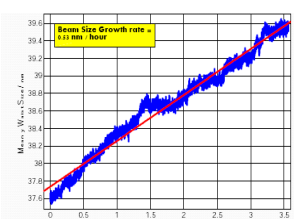


Figure 4: (a) Mean beam size growth as a function of time with orbit feedbacks only (b) Mean and RMS beamsize growth for a 2 week period with just feedbacks, periodic retuning of just linear and also non-linear sextupole knobs.

## SUMMARY

The next step for these tuning studies is to evolve the code developed into operational code that can be applied to the ATF2 machine. This will be done within the context of the flight simulator project- details of which can be found in these same proceedings.

## REFERENCES

- [1] B.I.Grishanov et. al., "ATF2 proposal. Vol. 2", KEK-REPORT-2005-9, Feb 2006.
- [2] T. Suehara et. al., "R&D Status of ATF2 IP Beam Size Monitor (Shintake Monitor)", arXiv:0709.1333v2, Sept. 2007.
- [3] G. Bowden, P. Holik, S. R. Wagner, "Precision Magnet Movers for the Final Focus Test Beam", SLAC-PUB-95-6132, June 1995.